A SPATIAL ANALYSIS OF HURRICANE KATRINA'S OUTER RAINBANDS PRIOR TO LANDFALL IN LOUISIANA

746

Corene J. Matyas *, Jingyin Tang, Ian J. Comstock, Stephanie E. Zick
University of Florida, Gainesville, Florida

1. INTRODUCTION

Much of the research on tropical cyclone (TC) rainbands explores convective cells within the eyewall given the importance of processes in this region for storm intensity (e.g., Jiang et al. 2012, Houze et al. 2006). However, rainbands located on the leading edge of a TC affect people hours before landfall, particularly in the case of large storms. Discussions with several attendees at the *Special Symposium on Hurricane Katrina: Progress in Leveraging Science, Enhancing Response and Improving Resilience* revealed stories of evacuees experiencing heavy rainfall on their drives out of New Orleans as Hurricane Katrina (2005) approached. One scientist believes that a tornado in one of these outermost convective cells touched down near his location although its presence was not confirmed by the National weather Service. In general, preparedness actions such as securing outdoor property and evacuating are hindered when rainfall commences, so it is important to define a rain start time.

This study focuses on the outer rainbands associated with Hurricane Katrina's (2005) Louisiana and Mississippi landfalls. Estimating the time when rain begins along the coastline allows a distance and time to be calculated relative to the arrival of the storm's center to provide a timeline for storm preparations to be completed. Measuring rainband shape, size, orientation, motion, and position relative to the storm center facilitates the examination of TC-environmental interactions and reveals how the outer edge of the TC changes during interaction with continental air masses and land. Our objectives are to 1) determine the hour when rainfall begins at coastal locations relative to the time of Katrina's landfall, and 2) track the position of the leading edge of the outermost rainband until data are no longer available from the radar located at Slidell, Louisiana.

2. DEFINING START OF RAINFALL EVENT

The hour of issuance for a TC warning conveys the time remaining until gale-force winds arrive, yet TC rainfall lacks this type of formal definition. Thus, our first task is to define the start time for each rainfall event. We examined hourly rainfall totals from the Stage IV gridded precipitation dataset (Fulton et al. 1998; Lin and Mitchell 2005), available online from the University Corporation for Atmospheric Research (http://data.eol.ucar.edu/codiac/dss/id=21.093). The advantage of using this dataset over the One Hour Precipitation product from Weather Surveillance Radar 1988 Doppler (WSR-88D) Level III is that Stage IV data are radar estimates that have been corrected using rain gauge totals and undergo quality control checks and analysis by personnel at the River Forecast Centers. The point data are gridded every 4 km and we interpolate these data using inverse distance weighting (Fig. 1). To our knowledge, there is not a widely accepted rain rate amount and duration threshold to define a rainfall event. For this study, we subjectively employ a minimum rain rate of 1.21 mm hr^{-1} that must be sustained for at least six hours. The rain event start time is the first hour of this qualifying six-hour period. Previous studies have used radar reflectivity values of 20 and 25 dB*Z* to define the edges of TC rainbands (Barnes et al. 1983; Cecil et al. 2002; Marks 1985; Matyas 2007), and 1.21 mm hr^{-1} equates to a 25 dB*Z* value using the tropical *Z* to *R* conversion equation ($Z=250R^{1.2}$; Rosenfeld et al. 1993).

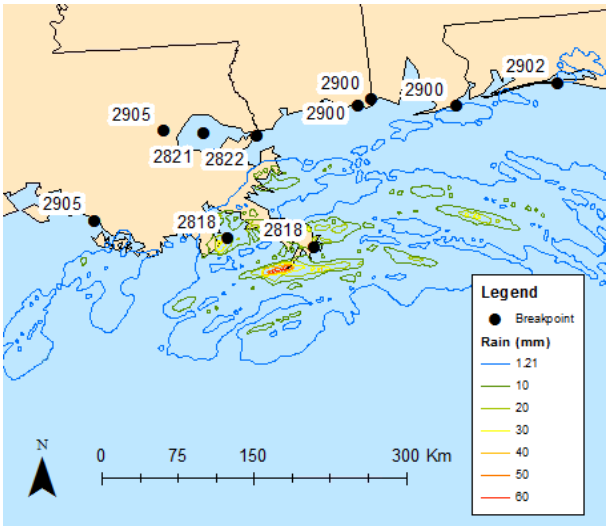

Fig. 1. Stage IV one-hour rainfall at 28 Aug. 1800 UTC. NHC breakpoint positions are labelled with day and time of rain event start.

The results we report here are part of a larger study that examined all U.S. landfalling TCs 2002-2012. To provide analysis at coastal locations also named in NHC advisories, we examined rainfall at all breakpoints (http://www.nhc.noaa.gov/breakpoints.php) affected

* *Corresponding author address:* Corene J. Matyas, Univ. of Florida, Dept. of Geography, Gainesville, FL 32611-7315; e-mail matyas@ufl.edu

by a given TC. The preliminary results of that study were presented by Comstock and Matyas (2014). We have investigated multiple thresholds to define rain events, but do not present those results here.

3. MEASUREMENTS OF WSR-88D REFLECTIVITY

We use the Level-III product NCZ (composite reflectivity of 460km range) from the eight radars closest to the location of Katrina's center during the study period to create a time series of large domain mosaics for Katrina. The spatial resolution is 4km. At every 5 minutes (e.g. 1200 UTC Aug. 29th) the NCZ products from each radar whose timestamp is closest to the mosaicking time are collected. The collected NCZ products are converted to NetCDF Version 4 format. Each NetCDF file contains one reflectivity image from one radar station. The NetCDF files are then rendered into a raster layer with 4km resolution using Albers equal-area conic projection with origin points located at the radar station, then inverse-projected back to the latitude-longitude coordinate. The rendered raster layers are merged into a single mosaic.

After we obtain a reflectivity mosaic, contour polygons of reflectivity are calculated from 15 dB*Z* to 45 dB*Z* with a 5 dB*Z* interval. For each polygon, its shape metrics are calculated including size, compactness, and position relative to storm center (Matyas 2008, Matyas et al. 2015). We also calculate the degree of closure as compared to a circle using the azimuthal coverage of the polygon under eye-centric polar coordinate system (Matyas 2007, Matyas and Tang 2014). Coordinates of the eye required in the calculations are interpolated from HURDAT and adjusted by hand when necessary using the radar signatures.

The next step is to identify the center lines for polygons containing reflectivity values of 40 dB*Z*, and to extract the outermost line at the top of each hour for this particular study. Smaller arcs located within close proximity to one another are joined together to create one larger line. We then compute the start, midpoint, endpoint, and length of lines, and measure the distance to a) the storm center and b) the nearest point on coastline. Results are reported in this study each hour 28 Aug. 1800 – 29 Aug. 1400 UTC.

4. EXAMINATION OF ENVIRONMENTAL MOISTURE

The availability of atmospheric moisture is key to the maintenance of a TC's circulation and rainbands. Papers by Hill and Lackmann (2009) and Matyas and Cartaya (2009) show that TCs can grow larger in size and produce more rainfall in their outer rainbands when relative humidity values are higher in the environment surrounding the TC. In this study, we explore the moisture surrounding Katrina using precipitable water data available every three hours from the North American Regional Reanalysis (NARR) (Mesinger et al. 2006). We selected this dataset as Zick and Matyas (2015 a, b) found good representation of TC secondary circulation for locations close to the U.S. In particular, Zick and Matyas (2016) found that Katrina's precipitation fields as measured from NARR data changed shape 24 hours prior to landfall, 6 h before reaching peak intensity, consistent with structural changes reported in Beven et al. (2008). We analyze precipitable water data beginning at 1800 UTC on 28 Aug.

4. RESULTS AND DISCUSSION: RAIN EVENT TIMING

For the ten breakpoints we examine during Katrina's Louisiana and Mississippi landfalls, we find that on average, rainfall begins 15 h prior to landfall when the TC center is 350 km away (Table 1). To place the findings from Katrina into context, we compare with the previously identified rainfall onset at coastal locations for 42 landfalling TCs 2002-2012. In this larger sample, the average rainfall onset occurs 12 h prior to landfall when the TC is 250-300 km from the breakpoints (Fig. 2). Katrina is large in size, with a radius of outermost closed isobar (ROCI) 555 – 650 km according to data from the extended best track file (Demuth et al. 2006). This places Katrina in the 90th percentile for the Atlantic basin TCs (Kimball and Mulekar 2004).

Breakpoint	Start Day Hour	Dist. to Center (km)	Avg. 6 hr Rain	Max. 6 hr Rain
Morgan City, LA	2905	255	3.30	5.02
Grand Isle, LA	2818	350	5.04	14.99
Mouth Miss. River	2818	320	3.14	8.85
Lake Maurepas, LA	2905	280	5.38	9.14
Lake Pontchartrain	2821	400	2.49	5.26
Mouth Pearl River	2822	375	1.98	3.14
Pascagoula, MS	2900	365	2.99	6.69
MS/AL border	2900	370	3.14	6.86
AL/FL border	2900	385	2.46	5.72
Destin, FL	2902	435	3.27	6.50

Table 1. Breakpoints, day and time of rain event start, distance from TC center at that time, average rainfall, and maximum rainfall over the 6-hr period used to calculate rain event start. Landfalls occur 29 Aug. at 1100 and 1445 UTC.

Given Katrina's large size, it is not unexpected that rainfall begins earlier than for other TCs (Fig. 2). In many cases, rainfall commences the earliest at

breakpoints that are located underneath the edges of the TC rather than directly in front of its path. This pattern is strongly evident when TC-breakpoint distances are grouped according to the type of wind warning that the breakpoint was experiencing at the time of rainfall start. Breakpoints under hurricane warnings are more likely to be close to the landfall point, while those under a tropical storm warning tend to be located farther from the eventual landfall point on either side of the storm track.

We also find that rainfall began at some breakpoints prior to the arrival of the radius of gale-force winds (R17). Analysis performed by Guo and Matyas (2016) showed that R17 averaged 300 km in the northern quadrants before reaching land on 28 Aug. McTaggart-Cowan et al. (2007) also show that 17 ms^{-1} winds had not reached the coastline at the time when the current study determines that rainfall commences at MS and AL breakpoints. Thus, rainfall can begin several hours before the arrival of gale-force winds, especially in locations not directly ahead of the TC. This shortens the time to complete storm preparations.

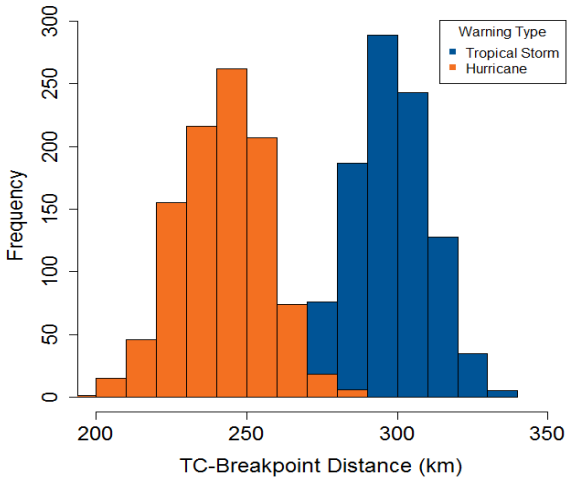

Fig. 2. Distance from TC center to breakpoint at rain event start for 42 TCs. Observations are grouped according to whether breakpoint is under a hurricane or TS warning at rain event start.

More work should be performed to examine the conditions under which rain events begin prior to the arrival of R17. Currently, we are developing a statistical model utilizing environmental conditions and storm characteristics to predict the distance at which a given breakpoint is from the TC center at rainfall start time. Comstock and Matyas plan to submit this manuscript in 2016 to *Weather and Forecasting*. We will also examine cases where rainfall start occurs more than six hours ahead of R17, which we hypothesize will be due to weak TCs in high-shear environments where moisture is abundant.

5. RESULTS AND DISCUSSION: MEASURING LEADING EDGE AND MOISTURE DISTRIBUTION

During the 20 h study period, we identify five main regions that we consider to be a leading edge of the rain field. At the time of the first analysis (1800 UTC 28 Aug.), the edge closest to land (Edge A) is located near the mouth of the Mississippi River (Fig. 3). It extends and curves towards the southwest on the other side of its center point. Edge A travels 250 km northwest before completely eroding, and the eastern edge erodes quickly after it crosses land. It has the fastest motion, averaging 22.5 ms^{-1}, and moves away from the circulation center after crossing land and becoming shorter in length (Fig 4). Edge C takes a similar trajectory 9 h later, moving at 15 ms^{-1}. It has the shortest length and it does not extend as far west as Edge A, yet it erodes at the same location.

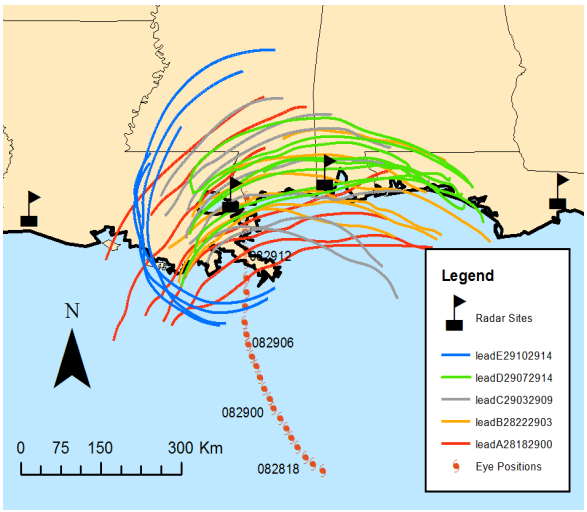

Fig. 3. Positions of 5 outer rainbands. Legend labels indicate day and hour of band formation and dissipation. TC centers are interpolated to each hour.

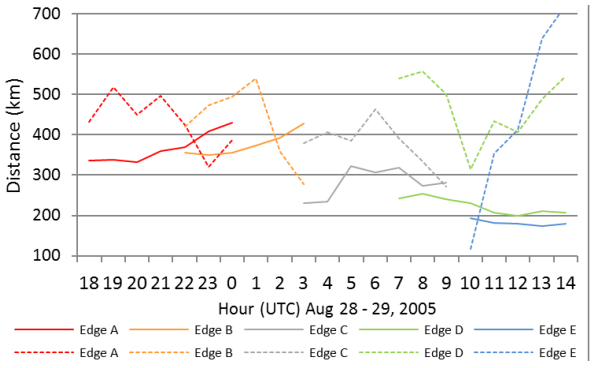

Fig. 4. Distance of each outer rainband from the circulation center (solid) and length of rainband (dashed) each hour.

Edge B forms over Lake Borgne at 2200 UTC and becomes the outermost rainband three hours later. Rather than moving northwest, Edge B moves north at an average speed of 14.4 ms^{-1}. Like Edge A, it moves farther away from the circulation center after its centroid crosses land and it decreases in length, although it erodes from the west. Edge D develops 9 hours later in a location similar to B along the Mississippi/Alabama coastline. It moves the shortest distance of 110 km, but has the longest length. Its forward motion averages 12.5 ms^{-1}.

At 1000 UTC on Aug. 29, Edge E forms 180 km west of the eye with a general north/south orientation. It encircles more than 180° around the eye within 5 hours, growing in length each hour from the shortest to the longest rainband. Like D, it moves slowly at 12.4 m s^{-1}. Despite its growth in extent, it maintains its distance from the eye and its edge remains in a similar location over Baton Rouge and Morgan City, Louisiana.

When examining the data across all five rainbands, three main trends emerge. First, earlier rainbands are located farther from the eye (A, B) and expand outwards as they decrease in length (Fig. 4). Data from the NARR show that precipitable water expands (Fig. 5 a, b), and data from the NHC shows that ROCI increases from 555 – 650 km during this time. This is likely due to expansion of the gale-force wind field as Katrina moves poleward. Increased convergence in the boundary layer as the forward edge of Katrina crosses land could also contribute to the expanding and increasing precipitable water field. Edge A forms along precipitable water values of 62 mm (Fig. 5a), while it dissipates along the gradient from 65 to 55 mm spanning 100 km (Fig. 5b). Edge B remains in the region of 62.5 mm values throughout its duration.

Second, Bands C, D, E form 300-180 km from the eye and maintain this distance. However, D and E grow in length towards the end. Like Edge B, Edges C and D remain in the region of 62.5 mm precipitable water values (Fig. 5c). Rainbands arched along the Mississippi/Alabama coastline move slowest, then move faster once crossing the coastline as they erode. The increased friction at the coastline might play a role in slowing forward progress. Additional studies should explore jointly the roles of frictional convergence and moisture gradients. Edge E does not expand away from the storm, but remains near 65 mm precipitable water values that form a gradient 65 – 45 mm spanning 200 km (Fig. 5d). It is an interesting observation that this is the only outer band that grows in extent as it remains nearly stationary.

Third, we find that two of Katrina's outermost rainbands with centroids located on the left side of the track exist on the inside of a moisture gradient of 1 mm per 10 km. The ability of NARR to accurately represent atmospheric moisture is somewhat limited given its 32 km horizontal resolution and the fact that it develops Katrina's intensity approximately six hours too late (Fig. 5b). However, the confluence of Katrina's counterclockwise circulation on the left side of the circulation center with the somewhat drier air from the continental air mass could be responsible for this gradient that appears to limit rain field expansion. Examination of specific humidity data from NARR at multiple levels (not shown) depicts the driest air, and therefore sharpest contrast between Katrina's circulation and the continental air mass, to occur in the middle troposphere at 500 hPa. Future research should identify similar gradients in moisture between TCs and their surrounding environments to determine if these regions tend to hinder the development of outer rainbands.

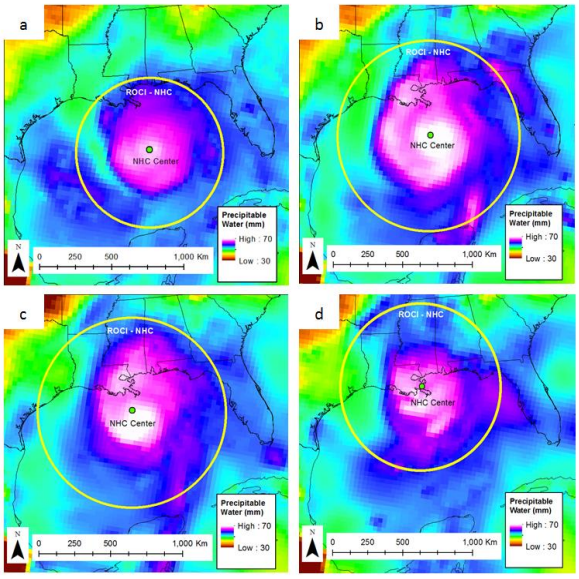

Fig. 5. Precipitable water from NARR at a) 28 Aug. 1800, b) 29 Aug. 0000, c) 29 Aug. 0600, and d) 29 Aug. 1200 UTC. Position of center and radius of outermost-closed isobar (ROCI) reported by NHC are indicated. Katrina's maximum intensity occurs at a, but NARR analysis (Zick and Matyas 2015a) shows it occurring at b, explaining the increasing amount and extent of precipitable water.

6. CONCLUSIONS AND FUTURE RESEARCH

We utilized multiple datasets derived from radar reflectivity values to define the start time of rainfall as Hurricane Katrina approached landfall. We also measured the spatial attributes of its leading edge during its landfalls on 29 Aug, 2005. Using a minimum rain rate of 1.21 mm hr^{-1} sustained for at least six hours to define a rainfall event, we found that rainfall commenced an average of 15 hours prior to landfall at 10 NHC breakpoints along the coast. Comparisons of this timing to previous research of Katrina's wind field and conversations with TC researchers who evacuated New Orleans during this period concur that rainfall commenced prior to the onset of damaging winds. Rainfall also commenced while the TC center was farther away from each breakpoint than the

majority of observations collected for 42 other U.S. landfalling TCs. Future research will explore additional reflectivity threshold and duration requirements to define a rain event and develop statistical models to explore the conditions under which rainfall develops when TCs are farther versus closer to each breakpoint. We will also estimate when R17 crosses land and explore the conditions under which rainfall commences hours prior to this time.

We then utilized composite reflectivity data to track the evolution of Katrina's leading rainbands over a 20 h period. We defined five rainbands that experienced different patterns of evolution in terms of their longevity, speed, trajectory, changes in length, and motion relative to Katrina's eye. Precipitable water values obtained from the NARR showed that these rainbands existed within regions of 62-63 mm. Rainband A eroded once it reached a 1 mm per 10 km gradient in precipitable water northwest of Katrina's center, while Rainband E persisted over land along the edge of a similar gradient west of center where counterclockwise flow from Katrina was converging with the drier continental air mass. Our future work will further explore moisture gradients along the outer edges of TC circulations as they approach and move over land. We have also developed automated algorithms to place Level II reflectivity and velocity data onto 3D grids (Tang and Matyas 2016) that will allow us to more precisely calculate shape metrics for numerous reflectivity values. This will facilitate our ongoing efforts to explore the growth and decline of rainfall regions of landfalling TCs.

7. REFERENCES

Barnes, G. M., E. Zipser, D. Jorgensen, and F. D. Marks, 1983: Mesoscale and convective structure of a hurricane rainband. *Journal of the Atmospheric Sciences*, **40**, 2125-2137.

Beven, J. L., and Coauthors, 2008: Atlantic hurricane season of 2005. *Monthly Weather Review*, **136,** 1109-1173. DOI:10.1175/2007mwr2074.1

Comstock, I. J., and C. J. Matyas, 2014: The timing of hurricane rain events along the coastal United States. *94th American Meteorological Society Annual Meeting*, Atlanta, GA.

Fulton, R. A., J. P. Breidenbach, D. J. Seo, D. A. Miller, and T. O'Bannon, 1998: The WSR-88D rainfall algorithm. *Weather and Forecasting*, **13,** 377-395.

Guo, Q., and C. Matyas, 2016: Comparing the spatial extent of Atlantic basin tropical cyclone wind and rain fields prior to land interaction. *Physical Geography*, DOI: 10.1080/02723646.2016.1142929

Hill, K., and G. M. Lackmann, 2009: Influence of environmental humidity on tropical cyclone size. *Monthly Weather Review*, **137**, 3294-3315.

Houze, R. A., and Coauthors, 2006: The hurricane rainband and intensity change experiment. *Bulletin of the American Meteorological Society*, **87**, 1503-1518.

Jiang, H., E. M. Ramirez, and D. J. Cecil, 2012: Convective and rainfall properties of tropical cyclone inner cores and rainbands from 11 years of TRMM data. *Monthly Weather Review*, **141**, 431-450.

Kimball, S. K., and M. S. Mulekar, 2004: A 15-year climatology of North Atlantic tropical cyclones. Part I: Size parameters. *Journal of Climate*, **17,** 3555-3575. DOI: 10.1175/1520-0442(2004)017<3555:AYCONA>2.0.CO;2

Lin, Y., and K. E. Mitchell, 2005: The NCEP Stage II/IV hourly precipitation analyses: development and applications. *85th Annual Meeting of the American Meteorological Society*, San Diego, CA.

Matyas, C. J., 2007: Quantifying the shapes of US landfalling tropical cyclone rain shields. *Professional Geographer*, **59,** 158-172. DOI: 10.1111/j.1467-9272.2007.00604.x

Matyas, C.J. , 2008: Shape measures of rain shields as indicators of changing environmental conditions in a landfalling tropical storm. *Meteorological Applications*, **15,** 259-271. DOI: 10.1002/met.70

Matyas, C. J., 2009: A spatial analysis of radar reflectivity regions within Hurricane Charley (2004). *Journal of Applied Meteorology and Climatology*, **48,** 130-142. DOI: 10.1175/2008jamc1910.1

Matyas, C. J., and J. Tang, 2014: Measuring the degree of closure of tropical cyclone outer rainbands and inner core. *Association of American Geographers Annual Meeting*, Tampa, FL

Matyas, C. J., J. Tang, and S. E. Zick, 2015: Performing spatial analysis on tropical cyclone rainband structures after creating a 3D Mosaic of WSR-88D reflectivity data using a map-reduce framework and a Geographic Information System (GIS). *37th conference on Radar Meteorology*, Norman, OK.

McTaggart-Cowan, R., L. F. Bosart, J. R. Gyakum, and E. H. Atallah, 2007: Hurricane Katrina (2005). Part I: Complex life cycle of an intense tropical cyclone. *Monthly Weather Review*, **135,** 3905-3926. DOI: 10.1175/2007mwr1875.1

Mesinger, F., and Coauthors, 2006: North American regional reanalysis. *Bulletin of the American*

Meteorological Society, **87,** 343-360. DOI: 10.1175/bams-87-3-343

Rew, Russ, and G. Davis, 1990: NetCDF: an interface for scientific data access. *Computer Graphics and Applications*, **10**, 76-82.

Rosenfeld, D., D. B. Wolff, and D. Atlas, 1993: General probability-matched relations between radar reflectivity and rain rate. *Journal of Applied Meteorology*, *32*, 50-72.

Tang, J., and C. J. Matyas, 2016: Fast playback framework for analysis of ground-based Doppler radar observations using Map-Reduce technology. *Journal of Atmospheric and Oceanic Technology*, accepted Jan. 28.

Zick, S. E., and C. J. Matyas, 2015a: Tropical cyclones in the North American Regional Reanalysis: An assessment of spatial biases in location, intensity, and structure. *Journal of Geophysical Research-Atmospheres*, **120**, 1651-1669. DOI: 10.1002/2014JD022417

Zick, S. E., and C. J. Matyas, 2015b: Tropical cyclones in the North American Regional Reanalysis: The impact of satellite derived precipitation over-ocean. *Journal of Geophysical Research-Atmospheres*, **120,** 8724-8742. DOI: 10.1002/2015JD023722

Zick, S. E., and C. J. Matyas, 2016: A shape metric methodology for studying the evolving geometries of synoptic-scale precipitation patterns in tropical cyclones. *Annals of the Association of American Geographers*, under review.